Journal of Materials Chemistry A

Accepted Manuscript

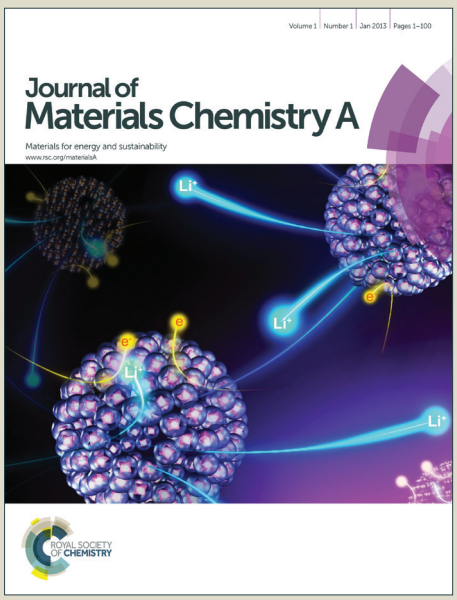

ROYAL SOCIETY OF CHEMISTRY

www.rsc.org/materialsA

Journal Name

RSCPublishing

ARTICLE

Pt-free Transparent Counter Electrodes for Cost-effective Bifacial Dye-sensitized Solar Cells

Cite this: DOI: 10.1039/x0xx00000x

Qidong Tai*[a], Xing-Zhong Zhao*[b]

Received 00th January 2012,
Accepted 00th January 2012

DOI: 10.1039/x0xx00000x

www.rsc.org/

Bifacial dye-sensitized solar cells (DSCs) that are able to utilize the incident light from both front-and rear-side, have received increasing attention in very recent years. Compared to conventional DSCs that can only be operated under front-side illumination, bifacial design will allow DSCs to generate up to 50 % more electrical power. Besides, bifacial DSCs can be easily made transparent and may find broad applications in building integrated photovoltaics (BIPV) as power-generating windows and roof panels. Transparent counter electrodes (CEs) are the key to the fabrication of bifacial DSCs. Despite the conventional Pt CE can be made transparent, its high cost and scarce source may hinder the large-scale application of DSCs. Therefore, many efforts have been made to develop low-cost alternative CEs based on carbon materials, conducting polymers, inorganic compounds and their composites. In this feature article, we intend to pay a special attention to the recent advances in the development of Pt-free transparent CEs and highlight their applications in bifacial DSCs.

1. Introduction

With advantages of low-cost, easy-fabrication and reasonable conversion efficiency, Dye-sensitized solar cells (DSCs) offer a promising alternative to conventional Si-based photovoltaic devices.[1-3] State-of-art DSC is composed of a mesoporous TiO_2 film covered by a monolayer of sensitizer (dye-sensitized photoanode), an electrolyte containing a redox couple e.g. I^-/I_3^- used as a mediator in regenerating the sensitizer and a counter electrode (CE) typically made of platinized fluorine-doped SnO_2 (FTO) glass.[4, 5] As one of the basic components of DSCs, the CE functions to catalyze the reduction of oxidative species in the electrolyte by passing them electrons collected from external circuit, therefore, a competent CE material should be of sufficient conductivity and catalytic activity to fulfill such a function.[4-6]

When DSC works, if the incident light is introduced through the photoanode, it is called front-side illumination; if through the CE, it is then called rear-side illumination. DSCs that are able to work under either front- or rear-side illumination are referred as bifacial DSCs[7] (see figure 1). With the ability to utilize the incident light from both sides, bifacial design is a smart way to improve the power generation efficiency of DSCs.[7, 8] Compared to conventional DSCs that can only be operated under front-side illumination, bifacial DSCs are able to generate up to 50% more electrical power, especially when the they are applied with reflecting devices.[9, 10] Besides, bifacial DSCs can be easily made transparent and may find broad applications in building integrated photovoltaics (BIPV) as power-generating windows and roof panels. Therefore, the development of bifacial DSCs is of great importance for the practical application of DSCs.

The fabrication of bifacial DSCs requires transparency of the CEs. And the characterization of bifacial DSCs is similar to conventional DSCs. Typically, the photovoltaic characteristics of a bifacial DSC are measured under front- and rear-side illumination separately and the device performance is evaluated by the front- and rear-side power conversion efficiencies (PCE_{front} and PCE_{rear}, respectively) and the PCE_{rear}/PCE_{front} ratio. For given photoanode and electrolyte, the PCE_{front} and PCE_{rear}/PCE_{front} ratio are mainly determined by the catalytic activity and the transparency of the CE. A well-performed bifacial DSC should exhibit both high PCE_{front} and PCE_{rear}/PCE_{front} ratio, which means high catalytic activity and transparency are both required for CEs.

Traditional Pt CE can be made transparent or semitransparent by reducing the amount of Pt deposited on FTO glass, and the first bifacial DSC was fabricated by Ito et al with a transparent

Pt CE and power conversion efficiency (PCE) of ~6% was obtained corresponding to front- or rear-side illumination.[7] However, Pt is not an ideal material for mass production of DSCs due to its scarce source and high cost (0.1g/m^2 Pt is needed in DSCs corresponding to 5nm film thickness which costs about 4.6 USD/m^2 without taking into account of the production cost and the methods used for preparing Pt CE are typically high energy-consuming).[11-13] On the other hand, the high reflectance of Pt film could also be a hinder for preparing high performance bifacial DSCs.[10] Tremendous efforts have been made to develop low-cost Pt-free CEs based on carbon materials,[14-16] conducting polymers,[17-19] inorganic compounds[20-22] and their composites [23-25] (the costs of these CEs, which vary with different materials and methods used for preparing them, are 10-10000 orders of magnitude lower than that of Pt CE), from which transparent Pt-free CEs are also expected. In this feature article, we intend to pay a special attention to the recent advances in Pt-free transparent CEs and highlight their applications in bifacial DSCs. In some cases, these CEs were not characterized under rear-side illumination but promising application of them in bifacial DSCs could still be expected.

2. Pt-free transparent counter electrodes

2.1. Carbon Materials

Carbon materials are the most extensively studied alternative CEs to Pt. However, in most cases, carbon-based CEs should be made very thick (typical in the range of 1-150 μ m) to get desired conductivity and catalytic activity which obviously makes them optically nontransparent.[14, 26-30] It was found that a CNT film with a transmittance of 40% at 550nm (T_{550} = 0.4) could exhibit comparable charge transfer resistance (Rct) (1.8 Ωcm^2) for the reduction of I_3^- to ~10-20μm opaque carbon black films. However, the Rct values were increased to 4.2 and 13.5 Ωcm^2 corresponding to thinner CNT films with higher transmittance of 74% and 88%, respectively. Nevertheless, these CNT films were not tested in DSCs.[31] In a similar study, Lee et al showed that transparent CNT CEs could be simply prepared by reducing the film thickness, but a compromise in the device performance was inevitable.[32] Realizing that it was naturally difficult to simultaneously obtain high transparency and good catalytic activity from conventional CNTs, Cha and coworkers proposed to prepare highly transparent CNT CEs by using CNT micro-balls in which the CNTs were densely packed, so as to provide sufficient active area. Meanwhile, the transparency of the CNT film could be tuned by controlling the density of the CNT micro-balls. The PCE of DSC using such a CNT micro-balls CE approached 80% of that using Pt CE (6.37%) at T_{550} = 0.7.[33] Recently, Seo et al prepared a highly transparent (T_{550} = ~0.8) CE by self-assembly of single-walled CNT (SWNT) on FTO substrate, which showed a PCE of ~4.7% under front- or rear-side illumination in a $[Co(bpy)_3]^{3+/2+}$(bpy = 2,2'-bipyridine) mediated bifacial DSC (figure 2).[34] The method they used seems to be an attractive way to prepare transparent CNT electrodes with high catalytic activities.

Graphene, a 2-dimentional allotrope of carbon, is believed to be a promising electrode material for electronic devices, due to its excellent conductivity and transparency.[35] However, it is recognized that defect-free bulk graphene is not an ideal CE material for lacking of active sites, which could be a limiting factor for preparing transparent graphene CEs.[12, 30] Instead of using bulk graphene, small graphene nanoplatelets (GNP) that have large number of active edges, were proposed for better catalytic activity. And PCEs of ~5% were obtained with highly transparent CEs (T_{550} = 0.87) prepared from GNPs, which were over 70% that of Pt-based device.[30] Though these CEs were not tested under rear-side illumination, their promising application bifacial DSCs can still be expected. In another study, nitrogen-doping was used to prepare highly catalytic and transparent graphene CEs, which produced PCEs of 6.12% and 5.23% under front- and rear-side illumination, respectively, at T_{550} = 0.77. In comparison, a PCE of 6.89% was achieved with Pt CE under the same condition.[36] Besides, reduced graphene oxide (RGO) was also used to prepare transparent CEs for DSCs, but the performance was much lower than Pt CEs.[37, 38] Typically, it is hard for graphene based CEs to achieve comparable performance to Pt CE in I-mediated DSCs for graphene's intrinsic low catalytic activity for I_3^- reduction.[12] However, performance comparable or even superior to Pt CE is achievable for graphene CEs in Co-mediated DSCs.[39-41] PCEs > 9% were achieved with transparent GNP CEs (T_{550}=0.66) in DSCs using $[Co(bpy\text{-}pz)_2]^{3+/2+}$ (bpy-pz = 6-(1H-pyrazol-1-yl)-2,2'-bipyridine) or $[Co(bpy)_3]^{3+/2+}$ redox couple in combination with a triphenylamine based dye coded Y123, which were higher than that (~8%) obtained with Pt CE (figure 3a, b).[39,40] however, one big problem for such CEs is the poor adhesion of GNP on FTO substrate, which would increase the dark current in DSCs and thus lower the open-circuit voltage, causing concerns for device's long-term stability. In a further study, this problem was solved by incorporating GO into GNP film, as the strong interaction of GO with FTO could dramatically improve the mechanic stability of graphene electrodes. The pristine GO exhibited almost no catalytic activity towards $[Co(bpy)_3]^{3+/2+}$ before heat treatment in inert atmosphere (GO-HT) or chemical reduction with hydrazine (RGO) was applied. The former treatment was found to be better and was used for the activation of GO/GNP CEs. The optimal GO/GNP CE was containing 50 wt% of GO, which led to PCEs of 9.1% and 9.3% under 1 sun front-side illumination at T_{550} = 0.8 and 0.69 (according to different carbon loading), respectively, almost the same as that achieved with pure GNP CEs. Besides, an 8.8% PCE was obtained with pure GO-HT CE of T_{550} as high as 0.86, comparable to 9.0% of Pt CE (figure 3c, d).[41] These efficiencies are much higher than that obtained with similar CEs in I-mediated DSCs, suggesting the importance of good match between CEs and redox couples,[12, 42] highlighting the prospect for preparing highly efficient Co-mediated bifacial DSCs with transparent graphene CEs.

Apart from the carbon-based transparent CEs mentioned above, our group has developed a novel transparent carbon CE with excellent catalytic activity and mechanic stability by in situ carbonization of an organic precursor coating on FTO glass in argon atmosphere (figure 4) at 500 ℃. Under optimal condition, carbon CEs with ~ 70% transparencies over the whole visible spectrum were prepared and used to fabricate bifacial DSCs. The best performing device showed a PCE_{front} of 6.07%, which was slightly lower than that using Pt CE (6.89%), while the PCE_{rear} (5.04%) approached 85% that of front-side illumination (figure 4). Due to the good connection between the carbon layer and FTO, the device also exhibited promising long-term stability. [43] This work provides a new solution for preparing high performance transparent carbon CEs and better results are expected by further optimizing the composition of the organic precursor.

In summary, CNT and graphene can be used to prepare transparent CEs, but their catalytic activities are strongly dependent on the film thickness when the I_3^-/I^- electrolyte is used, which will blur their applications in I-mediated bifacial DSCs. In contrast, promising applications of highly transparent CNT and graphene CEs in Co-mediated bifacial DSCs are highlighted. Interestingly, transparent carbon CE prepared by an in situ carbonization method has shown considerable performance in I-mediated DSC and its application in Co-mediated DSCs is expected.

2.2 Conducting Polymers

In recent years, conducting polymers such as polyaniline (PANI),[17, 44-49] polypyrrole (PPy),[18, 50-52] poly(3,4-ethylenedioxythiophene)(PEDOT)[53-57] and poly(3,4-propylenedioxythiophene) (PProDOT)[58-60] (figure 5) have drawn much attention as alternative CEs for DSCs for their excellent catalytic activities, good conductivity, low cost, easy preparation, low-temperature processability, flexibility as well as good transparency. Among them, PANI is most favorable for high performance bifacial DSCs, because it is quite transparent in visible region (that is complementary with most of the dyes used in DSCs) which helps to reduce the light loss on the rear side and its excellent catalytic activity and conductivity allow PANI film to be made as thin as possible to get high transparency.[17] It should be noted that PANI can exist in forms of leucoemeraldine (fully reduced state), emeraldine (half oxidized state) and pernigraniline (fully oxidized state), but only emeraldine PANI has shown appropriate catalytic acitivity and the conductivity of emeraldine PANI can be remarkably improved by acid doping.[44, 61] Therefore, acid doped emeradine PANI has been preferentially used for CEs in DSCs.

It was typically difficult to prepare PANI film via simple solution-based methods, due to PANI's poor solubility in most of the organic solvents. However, camphorsulfonic acid (CSA) doped PANI are soluble in m-cresol, which makes it possible to prepare transparent PANI CE by a facile spin-coating method.[45] Moreover, the CSA-doped PANI film prepared from m-cresol was found to exhibit excellent conductivity that enabled sung et al to prepare a transparent conductive oxide (TCO) free transparent PANI CE.[46] At optimized condition, the PANI CE presented promising PCE_{front} of 5.5% and PCE_{rear} of 2.67% in a bifacial DSC. In a study conducted by Zhang et al,[47] nanostructured PANI films were grown on FTO by cyclic voltammetry (CV) and the film thickness was controlled by changing the number of sweep segments i.e. the deposition time. The PANI film prepared with moderate sweep segments (25 segments) was quite transparent (the transmittance was not shown by the authors) and produced a PCE of 4.73% in DSC, which was just slightly lower than that of DSCs assembled with PANI CEs prepared with more sweep segments.

Our group has prepared a highly transparent PANI film (T_{550} = 0.7) on FTO by an in-situ chemical polymerization method and used it as CE to fabricate a bifacially active transparent DSC.[17] The as-prepared PANI film appeared quite uniform and smooth when looked with naked eyes, but showed a porous microstructure in nanoscale as revealed by SEM (figure 6a, b) which rendered it with high surface area and thus good catalytic activity that was comparable to Pt CE. Figure 6c shows the bifacial DSC prepared in our work, which gave a 6.54% PCE_{front} comparable to 6.69% of Pt-based device and the PCE_{rear} was 4.26% (figure 6d) approaching 65% that of front-side illumination. The high PCE_{rear}/PCE_{front} ratio benefited from the complementary absorption properties of PANI and N3 dye used in our work.

With a similar in-situ chemical deposition method as we used for preparing transparent PANI CE, transparent PPy CEs were also successfully fabricated in our group and PCEs of 5.74% and 3.06% were obtained with front- and rear-side illumination, respectively, compared to 6.76% of the device using Pt CE (figure 7).[18] Recently, ultrathin PPy nanosheets were synthesized and coated on FTO glass as CEs for DSCs in Im's lab.[51] With a T_{550} of ~0.6, the pristine PPy CE exhibited a 5.7% PCE, close to that obtained in our work. HCl vapor treatment was applied to improve the conductivity of the pristine PPy CE, which led to an increase of the PCE to 6.8%. However, the rear-side performance of the device was not shown in their work.

Though PEDOT is known for its good transparency, there are few reports presenting the application of transparent PEDOT CEs in (bifacial) DSCs. Pringle et al studied the electrodeposition of PEDOT on plastic ITO-PEN substrate as CEs for DSCs.[54] They found the electrochemical activity of PEDOT film increased linearly with deposition time (5-30s), but no significant influence of deposition time on the performance of DSC was observed. This phenomenon was explained by the sufficient electrochemical activity of PEDOT CE that was no more a limiting factor in determining the efficiency of DSC. It is thus can be inferred that with short deposition time (<10s), transparent PEDOT CEs are available for bifacial DSCs. Han et al demonstrated a bifacial DSC with a highly transparent electrodeposited PEDOT CE (transmittance > 91%) and a new thiolate/disulfide (AT^-/BAT) electrolyte.[62] The new redox couple AT^-/BAT was designed to replace the traditional I^-/I_3^- couple, which has strong absorption in the visible region and thus hinders the rear-side efficiency of

bifacial DSCs (figure 8a). With advantages of transparent PEDOT CE and colorless electrolyte, the device showed PCEs of 6.07% and 4.35% according to front- and rear-side illumination, respectively. In comparison, the I^-/I_3^- electrolyte was also tested, and a lower PCE_{rear} was obtained (3.93%) (figure 8b). Except for increasing the transparency of CEs, Han's work proved the reduction of the light loss in electrolyte (by developing colorless iodine-free electrolyte) was also an efficient way to improve the rear-side efficiency of bifacial DSCs.

Park et al reported a Pt- and TCO-free CE based on highly conductive (800 S/cm) PEDOT film prepared by pre-solution/in situ polymerization method. A thin PEDOT film of ~60 nm thickness showed a surface resistivity of 130 Ω/□ and a T_{550} = 0.88, gave a PCE of 5.08% in DSC which was comparable to Pt CE (5.88%).[63] In a more recent work, Shiratori et al prepared a flexible, TCO-free, transparent CE by combining PEDOT/PSS and Ag network substrate, where the Ag network functioned as conductive layer, while the PEDOT:PSS served as both catalyst and barrier against the corrosion of Ag from iodine. With transmittance of ~60% at 450nm, the CE did not perform well in DSCs, only 1.02% and 0.61% PCEs were obtained for front- and rear-side illumination, respectively, for the lack of catalytic surface. After incorporating TiO_2 nanoparticles into the PEDOT:PSS layer, the PCE_{front} was remarkably improved to 5.13%, which was close to 5.36% of Pt-based DSC. However, the influence of TiO_2 on the transparency of the CE was not mentioned.[64]

Although encouraging progress has been made towards the development of cost-effective transparent polymer CEs for bifacial DSCs, there are still much efforts need to be done before they can be used in practical applications, including the stability test, development of flexible and TCO-free polymer CEs as well as the seeking of new polymers with better performance than current ones.

2.3. Inorganic compounds

Recently, inorganic metal compounds including sulfides,[20, 65-72] carbides,[21, 22] nitrides,[22, 73] and oxides[22, 74] are emerging as a new class of Pt-free CEs for DSCs. Among numbers of papers that have been published, only a few of sulfides were reported to be able to be made transparent. Meng et al for the first time prepared a transparent electrodeposited NiS CE with a periodic potential reversal (PR) technique,[65] which yielded a 6.82% PCE in DSC employing I^-/I_3^- electrolyte that competed with Pt CE (7%). However, the performance of this kind of NiS CE, found by Han et al,[66] was insufficient in thiolate/disulfide mediated DSCs (PCE = 4.1%). By changing the PR period from 10 to 1, they produced a highly transparent (T_{550} = 0.9) NiS CE containing more content of sulfur, which showed better catalytic activity towards the thiolate/disulfide redox couple, resulting in a much higher PCE of 6.25%. Lin et al did serial research to prepare transparent CEs with CoS nanosheets and $NiCo_2S_4$ nanoparticles,[67-69] which were general of transmittance of 60-80%, yielding PCEs around 6%, which were comparable to that of DSCs using Pt CEs.

In a study by Li et al,[70] the morphology dependence of MoS_2 transparent CEs was investigated with multi-layered MoS_2 (ML- MoS_2) sheets, few-layered MoS_2 (FL- MoS_2) sheets and MoS_2 nanoparticles (MoS_2 -NPs). They found, FL- MoS_2, with the highest BET surface area, gave the lowest PCE (1.74%) in DSC, which was much lower than that of ML- MoS_2 (2.92%) and MoS_2-NPs (5.41%), respectively. It was proposed that the catalytically active sites of layered MoS_2 lay only on edges, therefore the ML- MoS_2 contained more active sites than FL-MoS_2 and the MoS_2-NPs composed of small particles of ML-MoS_2, had the largest number of active sites, which explained their performance in DSCs. However, with similar film thickness, the FL- MoS_2 CE showed the highest transparency. With high catalytic activity and moderate transparency, MoS_2-NPs CEs may have promising applications in bifacial DSCs. In order to improve the catalytic activity of MoS_2 CE, active edge sites were artificially created on MoS_2 atomic layers by patterning holes, which led to a dramatic improvement of the device performance from 2% to 5.8%. Besides, the transmittance of MoS_2 CE was also greatly enhanced (T_{550} = 0.7 vs. 0.8).[71] However, the method used for preparing hole-patterned MoS_2 CE is somewhat complicated.

In a recent work,[72] Chen et al prepared a semitransparent FeS_2 film (T_{550} = 0.6) from FeS_2 nanocrystal (NC) ink by spin-coating and used it as CE to fabricate a bifacial DSC (figure 9a). The as-synthesized FeS_2 NCs were covered by long alkyl chain ligands (oleic acid and oleylamine), which would impede the charge transport of FeS_2 CE. Thus, the FeS_2 CE was treated with ethanedithiol to remove the insulating ligands. And this led to an improvement of device performance from 5.74% to 7.31%, under front-side illumination, comparable to 7.52% of DSC using Pt CE (figure 9b). The corresponding PCE_{rear} was 4.17%, which approached 57% of that from front-side illumination (figure 9c). They also demonstrated a flexible transparent FeS_2 CE on ITO/PET substrate, which exhibited a 6.36% PCE in DSC (figure 9d). These results suggest the versatile application of FeS_2 in bifacial DSCs.

So far, the reported transparent CEs based on inorganic compounds are still limited to some sulfides such as NiS, CoS, MoS_2 and FeS_2, and most of them have not been tested in DSCs with rear-side illumination. Consequently, more study is expected to evaluate their performance in bifacial DSCs with illumination from both sides and explore new transparent CEs from carbides, nitrides and so on.

2.4. Composite Materials

Except for using the above-mentioned materials alone, composites of two or more of them were also used as CEs in DSCs.[11] Combing the advantages of all materials, composite CEs usually performed better than individuals. The strategy of using composite materials is especially beneficial for fabricating high performance transparent CEs. Because one big problem lies in the preparation of transparent CEs is that it is usually difficult to get desired transparency, conductivity and catalytic activity from a single material, which is supposed to be solved by using composite materials.

In 2008, Shi et al reported a transparent CE of graphene/PEDOT:PSS composite film, which showed a 4.5% PCE in DSC.[75] To the best of our knowledge, this is the earliest report of a Pt-free transparent composite CE. However, very little work has been done on the fabrication of Pt-free transparent composite CEs since then. Recently, Lin et al prepared a transparent MoS_2-graphene nanosheet (GNS) composite film by electrophoretic deposition and used it as CEs in DSCs.[76] The MoS_2-GNS CE showed a transmittance over 70 % in visible region and the DSC using this CE gave a PCE of 5.81%, which was higher than that of cells using MoS_2 CE (4.15%) and GNS CE (2.68%), comparable to Pt-based DSC (6.24%). The superior performance was achieved by the synergistic effect of the intrinsically high electrochemical activity from MoS_2 and facile electron transport from GNS. More recently, transparent PANI/RGO CE was fabricated by a two-step method, which involved a pre-polymerization of aniline onto GO and electrostatic deposition of them on FTO, followed by a chemical reduction of the PANI/GO film with hydroiodic acid. A 15min deposition time was found to be optimal, the corresponding PANI/RGO CE (T_{550} = 0.9) showed a PCE_{front} of 7.84% and a PCE_{rear} of 6.08% (PCE_{rear}/PCE_{front} = 0.78), compared to 6.7% and 4.63% (PCE_{rear}/PCE_{front} = 0.69) of PANI CE (T_{550} = 0.7) prepared under similar condition. The better performance of PANI/RGO composite CE was attributed to the improved transparency, conductivity and catalytic activity. Moreover, the stability of PANI CE was also improved after introducing RGO.[77]

One challenge of preparing high quality graphene CEs is their poor electronic connection to FTO substrates, which could undermine their performance in DSCs. To overcome this, Mendes et al introduced Ni NPs between graphene and FTO substrate where the Ni NPs helped to restore the graphene double bonds and thus improved electronic contact at graphene/FTO interface.[78] In their study, the transparent graphend/Ni CE was prepared by spray-deposition of oxidized GNP on Ni NPs decorated FTO, followed by thermal annealing under inert atmosphere. Both water and ethanol were used as solvents for the deposition of oxidized GNP. The graphene/Ni CEs prepared with both solvents showed similar PCEs in DSCs (7.51% in water vs. 7.54% in ethanol) that competed with Pt CE (7.45%) (figure 10), while the CE prepared with ethanol was more transparent than the one prepared with water (T_{550} = 0.92 vs. 0.81) due to the different solvation effect on oxidized GNP. Given there was no corrosion of Ni NPs was observed by the authors, this kind of CEs should be promising in real applications.

As discussed before, the performance of Pt-free CEs are often limited to their insufficient catalytic activity. To this point, small amounts of Pt nanoparticles (Pt NPs) (1-2 μ g/cm^2)[79,80] are often incorporated into these CEs to get better photovoltaic performance. The quantity of Pt used is almost an order of magnitude lower that of pure Pt CE (according to our calculation in previous section), which means a minor increase of the total cost of CEs. Therefore, though our focus is Pt-free transparent CEs, the progress of low-cost, Pt-loaded transparent composite CEs and their applications in bifacial DSCs is also reviewed.

By using an ionic liquid assisted sonochemical method, Su et al synthesized composites of CNT (MWNT, SWNT) supported Pt NPs and electrospayed them on FTO glass as CEs for DSCs.[81] The CNT/Pt composite CEs exhibited excellent catalytic activity for I_3^- reduction with a weak dependence on film thickness. With thickness of about 100nm, the MWNT/Pt CE showed a transparency of ~65% at 550nm, resulted in a PCE of 8.81% close to that of Pt-based DSC (8.84%), while the SWNT/Pt CE gave a ~70% transparency and a PCE of 8.52%. They also demonstrated a PCE as high as 8.43% with a flexible MWNT/Pt CE on ITO/PET substrate, but the transparency of the flexible CE was not illustrated. Wang et al reported a self-assembled monolayer of graphene/Pt as CE for DSC and a PCE of 7.66% was obtained.[82] Though not shown in their work, the transparency of the graphene/Pt CE was claimed by the authors. Recently, Choi et al also made an effort to prepare Pt-loaded graphene as transparent CEs for DSCs.[83] In their study, the graphene layer was grown by chemical vapor deposition, and then it was transferred onto FTO glass, followed by the deposition of Pt NPs using dry plasma reduction (DPR) under atmospheric pressure at near room temperature (figure 11a). The graphene/Pt composite film showed almost the same transparency (T_{550} = 0.8) as pure graphene film in the wavelength range 300-1000 nm (figure 11b). The bifacial DSC with such a graphene/Pt CE exhibited PCEs of 6.55% and 5.17% under front- and rear-side illumination, respectively (figure 11c). This low temperature processed graphene/Pt CEs should be possibly prepared on flexible substrates. Instead of sequential deposition of graphene and Pt, hybrid of GNP and PtNPs was prepared by using poly(oxyethylene)-segmented oligo(imide) (POE-imide) as dispersant and spin-coated on FTO to fabricate transparent GNP/Pt CEs (figure 11d,e). The DSC using such GNP/Pt CE reached an optimized PCE_{front} of 8% at 5:1 weight ratio of Pt (H_2PtCl_6) and GNP for optimized size and distribution of PtNPs, which was higher than 7.14% of Pt based cell. Meanwhile, the DSC maintained 88% of its efficiency (PCE_{rear} = 7.01%) when irradiated from rear side (figure 11f).[84] However, this method is not applicable to plastic substrates, since high temperature sintering is required to remove the dispersant. More recently, Kim et al fabricated a transparent GO/Pt composite CE, in which the Pt particles were deposited on the surface of GO by pulse current deposition. The corresponding DSC showed a 7.1% PCE.[85]

Peng et al spin-coated the composites of PANI/Pt on plastic ITO/PET substrates and used them as transparent CEs for flexible bifacial DSCs.[86] The PANI/Pt composite CE showed excellent transparency in visible region ($T_{550} \approx 0.7$) and produced PCEs of 5.4% and 4.0% in the corresponding DSC under front- and rear-side illumination, respectively, which were higher than that of Pt based device (5.1% and 3.8%). In a further work,[80] they prepared PANI/Pt CEs on FTO and investigated the influence of Pt loading on their catalytic performance with quasi-solid state DSCs using PVDF-HFP/TiO_2 electrolyte. They found a 1.5 μ g/cm^2 Pt loading was

enough to get high catalytic activity , which produced PCEs of 6.34% and 3.85% in the solid-state device under front- and rear-side illumination, respectively. Brown et al reported a highly transparent CoS/Pt composite CE (T_{550} = 0.8) for rear-illuminated DSC and bifacial DSC,[87] which was prepared by simultaneous electrodeposition of CoS and Pt on FTO from a mixture solution of both precursors. The bifacial DSC using such a CoS/Pt CE reached PCEs of 6.15% and 4.45% under front- and rear-side illumination, respectively, compared to 6.15 % and 4.15% of the device using electrodeposited Pt CE of similar transparency.

We noticed that graphene has been widely used as a functional component to prepare transparent composite CEs with other materials, which can be attributed to its excellent conductivity and transparency. It is noteworthy that though pure Pt CE is unfavorable in DSCs, the development of Pt-loaded CEs could be a practical option, as the amount of Pt needed is extremely low. Given the large number of CE materials, except for the composite CEs mentioned above, there should be far more possible combinations them, which are expected in future exploration.

3. Conclusions and Outlook

Bifacial DSCs that are able to harvest the incident light from both sides have attracted much attention in recent years, for their enhanced power generation efficiency and possibility to be made transparent for see-through applications, compared to state-of-art monofacial DSCs. CEs of good catalytic activity and transparency are crucial for the fabrication of efficient bifacial DSCs. Though conventional Pt CE can be made transparent, its application DSCs is unfavorable for its high cost and limited source. Many efforts have been made to prepare alternative transparent CEs based on carbon materials, conducting polymers, inorganic compounds and composites of them and some of them have shown promising applications in bifacial DSCs as listed in table 1.

Traditional carbon materials such as carbon black, activated carbon, mesoporous carbon are unlikely to be made transparent. CNTs and graphene can be used to prepare transparent CEs, however their performance is poor in conventional I-mediated DSCs for their intrinsic low catalytic activity towards the reduction of I_3^-. Better performance is expected by modification of them and/or by using other redox shuttles. Very encouraging results ($PCE_{front} \approx 9\%$) have already been achieved with transparent graphene based CEs in Co-mediated DSCs. Noticeably, in situ carbonization of organic precursor offers a promising way to prepare highly transparent carbon CE with excellent catalytic activity and mechanical stability. Conducting polymer such as PANI, PPy, PEDOT etc. are promising candidates for flexible and transparent CEs due to their excellent transparency, catalytic activity and low-temperature processability. Amongst kinds of inorganic compounds (sulfides, carbides, nitrides, oxides and phosphides) that have been explored as alternative CEs in DSCs, only a few of sulfides e.g. NiS, CoS, MoS_2 and FeS_2 have been made transparent. Further study is needed to figure out whether it is possible to prepare transparent CEs from other compounds. Except for using single material, the strategy of using composite materials offers new opportunity to fabricate high performance transparent CEs. And graphene has shown its versatile application in fabricating transparent composite CEs, for its good transparency and conductivity. It will be arbitrary to conclude which one these CEs is better than another since each of them is of unique advantages and worthy of further exploration.

However, most of these CEs have only been tested in I-mediated DSCs, study of them in DSCs using other redox couples is expected to see if there is any room for further improvement of the device performance, because a better match of them with other redox couples maybe possible and the light absorption of I_3^-/I^- electrolyte that will reduce the rear-illuminated efficiencies of DSCs could be overcome by using its colorless alternatives. Prior to real application, the long-term stability of these CEs in DSCs should be further explored especially for polymer-based CEs. Besides, the development of other low-cost transparent CEs and the preparation of these CEs on flexible and/or TCO-free substrates are also desired.

Acknowledgements

We gratefully acknowledge the financial support of this work by the National Basic Research Program of China (No. 2011CB933300).

Notes and references

[a] Institute for Interdisciplinary Research, Jianghan University, Wuhan 430072, P. R. China. Email: qdtai@hotmail.com
[b] School of Physical Science and Technology, Wuhan University, Wuhan 430072, P. R. China. Email: xzzhao@whu.edu.cn

1 A. Yella, H.-W. Lee, H. N. Tsao, C. Yi, A. K. Chandiran, M. K. Nazeeruddin, E. W.-G. Diau, C.-Y. Yeh, S. M. Zakeeruddin and M. Grätzel, *Science*, 2011, **334**, 629-634.
2 B. E. Hardin, H. J. Snaith and M. D. McGehee, *Nat. Photonics*, 2012, **6**, 162-169.
3 S. Mathew, A. Yella, P. Gao, R. Humphry-Baker, F. E. CurchodBasile, N. Ashari-Astani, I. Tavernelli, U. Rothlisberger, M. K. Nazeeruddin and M. Grätzel, *Nat. Chem.*, 2014, **6**, 242-247.
4 A. Hagfeldt, G. Boschloo, L. Sun, L. Kloo and H. Pettersson, *Chem. Rev.*, 2010, **110**, 6595-6663.
5 J. Halme, P. Vahermaa, K. Miettunen and P. Lund, *Adv. Mater.*, 2010, **22**, E210-234.
6 T. N. Murakami and M. Grätzel, *Inorg. Chim. Acta*, 2008, **361**, 572-580.
7 S. Ito, S. M. Zakeeruddin, P. Comte, P. Liska, D. Kuang and M. Grätzel, *Nat. Photonics*, 2008, **2**, 693-698.
8 J. Bisquert, *Nat Photonics*, 2008, **2**, 648-649.
9 R. Hezel, *Prog. Photovoltaics*, 2003, **11**, 549-556.

10 J. Wu, Y. Li, Q. Tang, G. Yue, J. Lin, M. Huang and L. Meng, *Sci Rep.*, 2014, **4**, 4028.
11 M. Wu and T. Ma, *ChemSusChem*, 2012, **5**, 1343-1357.
12 S. Ahmad, E. Guillen, L. Kavan, M. Gratzel and M. K. Nazeeruddin, *Energy. Environ. Sci*., 2013, **6**, 3439-3466.
13 F. Hao, P. Dong, Q. Luo, J. Li, J. Lou and H. Lin, *Energy. Environ. Sci.*, 2013, **6**, 2003-2019.
14 M. Wu, X. Lin, T. Wang, J. Qiu and T. Ma, *Energy. Environ. Sci.*, 2011, **4**, 2308-2315.
15 H. Wang and Y. H. Hu, *Energy. Environ. Sci.*, 2012, **5**, 8182-8188.
16 W. Kwon, J.-M. Kim and S.-W. Rhee, *J. Mater. Chem. A*, 2013, **1**, 3202-3215.
17 Q. Tai, B. Chen, F. Guo, S. Xu, H. Hu, B. Sebo and X.-Z. Zhao, *ACS Nano,* 2011, **5**, 3795-3799.
18 C. Bu, Q. Tai, Y. Liu, S. Guo and X. Zhao, *J. Power Sources*, 2013, **221**, 78-83.
19 Y.-H. C. Chung-Wei Kung, Hsin-Wei Chen, R. Vittala and Kuo-Chuan Ho, *J. Mater. Chem. A*, 2013, **1**, 10693-10702.
20 M. Wang, A. M. Anghel, B. Marsan, N.-L. Cevey Ha, N. Pootrakulchote, S. M. Zakeeruddin and M. Grätzel, *J. Am. Chem. Soc*., 2009, **131**, 15976-15977.
21 M. Wu, X. Lin, A. Hagfeldt and T. Ma, *Angew. Chem. Int. Ed.*, 2011, **50**, 3520-3524.
22 M. Wu, X. Lin, Y. Wang, L. Wang, W. Guo, D. Qi, X. Peng, A. Hagfeldt, M. Grätzel and T. Ma, *J. Am. Chem. Soc.,* 2012, **134**, 3419-3428.
23 P. Sudhagar, S. Nagarajan, Y.-G. Lee, D. Song, T. Son, W. Cho, M. Heo, K. Lee, J. Won and Y. S. Kang, *ACS Appl. Mater. Inter.*, 2011, **3**, 1838-1843.
24 W. Sun, T. Peng, Y. Liu, S. Xu, J. Yuan, S. Guo and X.-Z. Zhao, J. *Mater. Chem. A*, 2013, **1**, 2762-2768.
25 S. Yun, H. Zhang, H. Pu, J. Chen, A. Hagfeldt and T. Ma, *Adv. Energy. Mater*., 2013, **3**, 1407-1412.
26 H. Hu, B.-L. Chen, C.-H. Bu, Q.-D. Tai, F. Guo, S. Xu, J.-H. Xu and X.-Z. Zhao, *Electrochim. Acta*, 2011, **56**, 8463-8466.
27 K. Imoto, K. Takahashi, T. Yamaguchi, T. Komura, J.-i. Nakamura and K. Murata, *Sol. Energy Mater. Sol. Cells*, 2003, **79**, 459-469.
28 G. Wang, W. Xing and S. Zhuo, *J. Power Sources*, 2009, **194**, 568-573.
29 J. Han, H. Kim, D. Y. Kim, S. M. Jo and S.-Y. Jang, *ACS Nano*, 2010, **4**, 3503-3509.
30 L. Kavan, J. H. Yum and M. Grätzel, *ACS Nano*, 2010, **5**, 165-172.
31 J. E. Trancik, S. C. Barton and J. Hone, *Nano Letters*, 2008, **8**, 982-987.
32 E. Ramasamy, W. J. Lee, D. Y. Lee and J. S. Song, *Electrochem. Commun.*, 2008, **10**, 1087-1089.
33 S. I. Cha, B. K. Koo, S. H. Seo and D. Y. Lee, *J. Mater. Chem.*, 2010, **20**, 659-662.
34 S. H. Seo, M. H. Kim, E. J. Jeong, S. H. Yoon, H. C. Kang, S. I. Cha and D. Y. Lee, J. Mater. Chem. A, 2014, 2, 2592-2598.
35 S. Pang, Y. Hernandez, X. Feng and K. Müllen, *Adv. Mater.*, 2011, **23**, 2779-2795.
36 G. Wang, Y. Fang, Y. Lin, W. Xing and S. Zhuo, *Mater. Res. Bull.*, 2012, **47**, 4252-4256.
37 R. Cruz, D. A. Pacheco Tanaka and A. Mendes, *Sol. Energy*, 2012, **86**, 716-724.
38 H.-S. Jang, J.-M. Yun, D.-Y. Kim, D.-W. Park, S.-I. Na and S.-S. Kim, *Electrochim. Acta*, 2012, **81**, 301-307.
39 L. Kavan, J.-H. Yum and M. Grätzel, *Nano Lett.*, 2011, **11**, 5501-5506.
40 L. Kavan, J.-H. Yum, M. K. Nazeeruddin and M. Grätzel, *ACS Nano*, 2011, **5**, 9171-9178.
41 L. Kavan, J. H. Yum and M. Graetzel, *ACS Appl. Mater. Interfaces*, 2012, **4**, 6999-7006.
42 J. Burschka, V. Brault, S. Ahmad, L. Breau, M. K. Nazeeruddin, B. Marsan, S. M. Zakeeruddin and M. Grätzel, *Energy. Environ. Sci.*, 2012, **5**, 6089-6097.
43 C. Bu, Y. Liu, Z. Yu, S. You, N. Huang, L. Liang and X. Z. Zhao, *ACS Appl. Mater. Interfaces*, 2013, **5**, 7432-7438.
44 H. Sun, Y. Luo, Y. Zhang, D. Li, Z. Yu, K. Li and Q. Meng, *J. Phys. Chem. C*, 2010, **114**, 11673-11679.
45 S. S. Jeon, C. Kim, T. H. Lee, Y. W. Lee, K. Do, J. Ko and S. S. Im, *J. Phys. Chem. C*, 2012, **116**, 22743-22748.
46 S. H. Park, K.-H. Shin, J.-Y. Kim, S. J. Yoo, K. J. Lee, J. Shin, J. W. Choi, J. Jang and Y.-E. Sung, J. Photochem. Photobiol. A: Chem., 2012, **245**, 1-8.
47 J. Zhang, T. Hreid, X. Li, W. Guo, L. Wang, X. Shi, H. Su and Z. Yuan, *Electrochim. Acta*, 2010, **55**, 3664-3668.
48 F. Guo, H. Hu, Q.-D. Tai, B.-L. Chen, B. Sebo, C.-H. Bu, J.-H. Xu and X.-Z. Zhao, *J. Renewable Sustainable Energy*, 2012, **4**, 023109.
49 H. Wang, Q. Feng, F. Gong, Y. Li, G. Zhou and Z.-S. Wang, *J. Mater. Chem. A*, 2013, **1**, 97-104.
50 J. Wu, Q. Li, L. Fan, Z. Lan, P. Li, J. Lin and S. Hao, *J. Power Sources*, 2008, **181**, 172-176.
51 J. Xia, L. Chen and S. Yanagida, *J. Mater. Chem.*, 2011, **21**, 4644-4649.
52 D. K. Hwang, D. Song, S. S. Jeon, T. H. Han, Y. S. Kang and S. S. Im, *J. Mater. Chem. A*, 2014, **2**, 859-865.
53 S. Ahmad, J.-H. Yum, Z. Xianxi, M. Gratzel, H.-J. Butt and M. K. Nazeeruddin, *J. Mater. Chem.*, 2010, **20**, 1654-1658.
54 J. M. Pringle, V. Armel and D. R. MacFarlane, *Chem Commun*, 2010, **46**, 5367-5369.
55 J. Burschka, V. Brault, S. Ahmad, L. Breau, M. K. Nazeeruddin, B. Marsan, S. M. Zakeeruddin and M. Grätzel, *Energy. Environ. Sci.*, 2012, **5**, 6089-6097.
56 C.-W. Kung, Y.-H. Cheng, H.-W. Chen, R. Vittal and K.-C. Ho, *J. Mater. Chem. A*, 2013, **1**, 10693-10702.
57 L. Chen, J. Jin, X. Shu and J. Xia, *J. Power Sources*, 2014, **248**, 1234-1240.
58 K.-M. Lee, C.-Y. Hsu, P.-Y. Chen, M. Ikegami, T. Miyasaka and K.-C. Ho, *Phys. Chem. Chem. Phys*., 2009, **11**, 3375-3379.
59 K.-M. Lee, P.-Y. Chen, C.-Y. Hsu, J.-H. Huang, W.-H. Ho, H.-C. Chen and K.-C. Ho, *J. Power Sources,* 2009, **188**, 313-318.
60 S. Ahmad, J.-H. Yum, H.-J. Butt, M. K. Nazeeruddin and M. Grätzel, *ChemPhysChem*, 2010, **11**, 2814-2819.
61 H. D. Tran, J. M. D'Arcy, Y. Wang, P. J. Beltramo, V. A. Strong and R. B. Kaner, *J. Mater. Chem.*, 2011, **21**, 3534-3550.
62 X. Li, Z. Ku, Y. Rong, G. Liu, L. Liu, T. Liu, M. Hu, Y. Yang, H. Wang, M. Xu, P. Xiang and H. Han, *Phys. Chem. Chem. Phys.*, 2012, **14**, 14383-14390.
63 K. S. Lee, H. K. Lee, D. H. Wang, N. G. Park, J. Y. Lee, O. O. Park and J. H. Park, *Chem. Commun.*, 2010, **46**, 4505-4507.

64 I. Okada and S. Shiratori, *ACS Appl. Mater. Interfaces*, 2013, **5**, 4144-4149.
65 H. Sun, D. Qin, S. Huang, X. Guo, D. Li, Y. Luo and Q. Meng, *Energy. Environ. Sci.*, 2011, **4**, 2630-2637.
66 Z. Ku, X. Li, G. Liu, H. Wang, Y. Rong, M. Xu, L. Liu, M. Hu, Y. Yang and H. Han, *J. Mater. Chem. A*, 2013, **1**, 237-240.
67 J.-Y. Lin, J.-H. Liao and T.-C. Wei, *Electrochem. Solid-State Lett.*, 2011, **14**, D41.
68 S.-Y. Tai, C.-F. Chang, W.-C. Liu, J.-H. Liao and J.-Y. Lin, *Electrochim. Acta*, 2013, **107**, 66-70.
69 J.-Y. Lin and S.-W. Chou, *Electrochem. Commun.*, 2013, **37**, 11-14.
70 B. Lei, G. R. Li and X. P. Gao, *J. Mater. Chem. A*, 2014, **2**, 3919-3925.
71 J. Zhang, S. Najmaei, H. Lin and J. Lou, *Nanoscale*, 2014, **6**, 5279–5283
72 Y. C. Wang, D. Y. Wang, Y. T. Jiang, H. A. Chen, C. C. Chen, K. C. Ho, H. L. Chou and C. W. Chen, *Angew. Chem. Int. Ed.*, 2013, **52**, 6694-6698.
73 M. Wu, Q. Zhang, J. Xiao, C. Ma, X. Lin, C. Miao, Y. He, Y. Gao, A. Hagfeldt and T. Ma, *J. Mater. Chem.*, 2011, **21**, 10761-10766.
74 X. Lin, M. Wu, Y. Wang, A. Hagfeldt and T. Ma, *Chem. Commun.*, 2011, **47**, 11489-11491.
75 W. Hong, Y. Xu, G. Lu, C. Li and G. Shi, *Electrochem. Commun.*, 2008, **10**, 1555-1558.
76 J. Y. Lin, C. Y. Chan and S. W. Chou, *Chem. Commun.*, 2013, **49**, 1440-1442.
77 Y.-S. Wang, S.-M. Li, S.-T. Hsiao, H. Wei, S.-Y. Yang, H.-W. Tien, C.-C. M. Ma and C.-C. Hu, *J. Power Sources*, 2014, **260**, 326-337.
78 R. Cruz, J. P. Araújo, L. Andrade and A. Mendes, *J. Mater. Chem. A*, 2014, 2, 2028-2032.
79 G. H. Guai, Q. L. Song, C. X. Guo, Z. S. Lu, T. Chen, C. M. Ng and C. M. Li, *Sol. Energy*, 2012, **86**, 2041-2048.
80 S. Peng, L. Li, H. Tan, M. Srinivasan, S. G. Mhaisalkar, S. Ramakrishna and Q. Yan, *Electrochim. Acta*, 2013, **105**, 447-454.
81 H. Y. Chen, J. Y. Liao, B. X. Lei, D. B. Kuang, Y. Fang and C. Y. Su, *Chem. Asian J.*, 2012, **7**, 1795-1802.
82 F. Gong, H. Wang and Z.-S. Wang, *Phys. Chem. Chem. Phys.*, 2011, **13**, 17676-17682.
83 V. D. Dao, L. V. Nang, E. T. Kim, J. K. Lee and H. S. Choi, *ChemSusChem*, 2013, **6**, 1316-1319.
84 P.-T. Shih, R.-X. Dong, S.-Y. Shen, R. Vittal, J.-J. Lin and K.-C. Ho, *J. Mater. Chem. A*, 2014, **2**, 8742-8748.
85 H.-S. Jang, J.-M. Yun, D.-Y. Kim, S.-I. Na and S.-S. Kim, *Surf. Coat. Techn.*, 2014, **242**, 8-13.
86 S. Peng, J. Liang, S. G. Mhaisalkar and S. Ramakrishna, *J. Mater. Chem.*, 2012, **22**, 5308-5311.
87 F. De Rossi, L. Di Gaspare, A. Reale, A. Di Carlo and T. M. Brown, J. Mater. Chem. A, 2013, 1, 12941-12947.

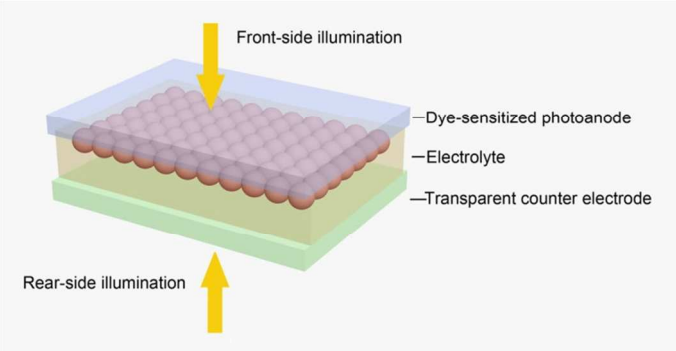

Fig.1 Illustration of a bifacial DSC

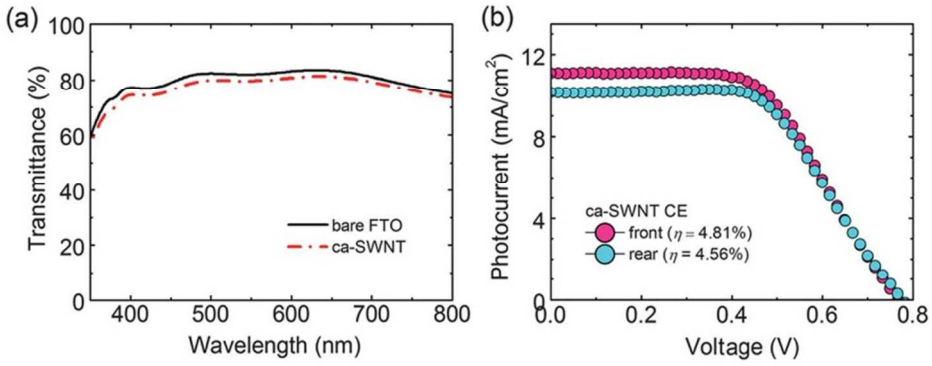

Fig.2 (a) Transmittance of FTO glass and ca-SWNT electrode, (b) J-V curves of bifacial DSC based on transparent ca-SWNT CE under front- and rear-side illuminations. Adapted from ref 34.

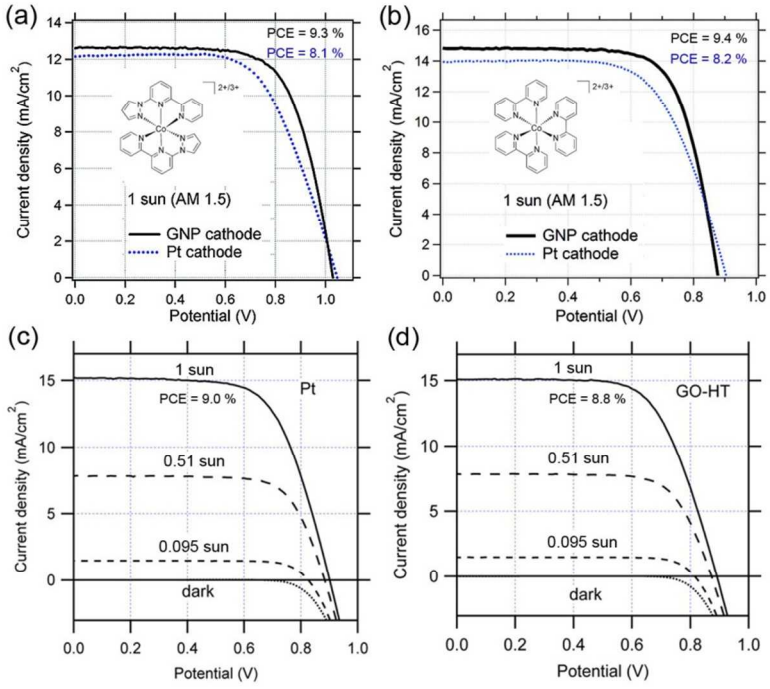

Fig.3 J-V characteristics of DSCs with different CEs, (a) GNP and Pt CEs using $[Co(bpy\text{-}pz)_2]^{3+/2+}$ redox couple (adapted with permission from ref 39. Copyright (2011) American Chemical Society.), (b) GNP and Pt CEs using $[Co(bpy)_3]^{3+/2+}$ redox couple (adapted with permission from ref 40. Copyright (2011) American Chemical Society.), (c) Pt CE and (d) GO-HT CE using $[Co(bpy)_3]^{3+/2+}$ redox couple. Adapted with permission from ref 41. Copyright (2012) American Chemical Society.

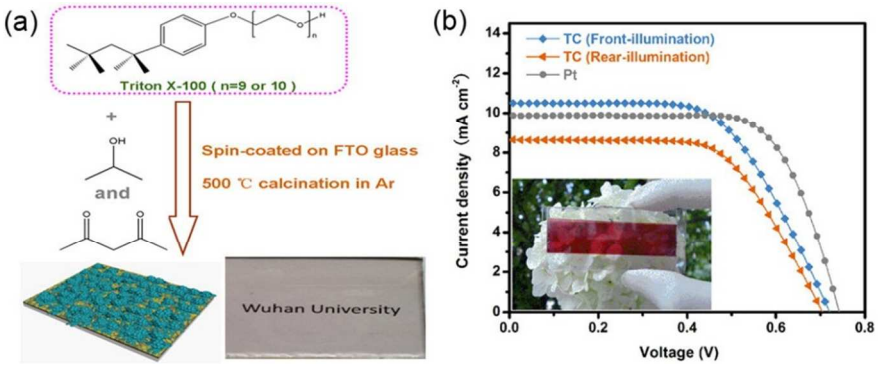

Fig.4 (a) Illustration of the preparation process and digital photograph of transparent carbon CE, (b) J-V curves of DSCs using transparent carbon CE and Pt CE, the inset shows a bifacial DSC fabricated with transparent carbon CE. Reproduced with permission from ref 43. Copyright (2013) American Chemical Society.

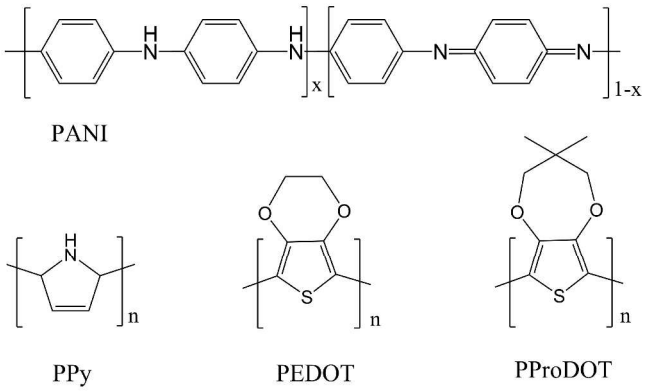

Fig. 5 Molecular structures of PANI (x = 1, 0.5, and 0 corresponds to PANI in leucoemeraldine, emeraldine , and pernigraniline state, respectively), PPy, PEDOT, and PProDOT.

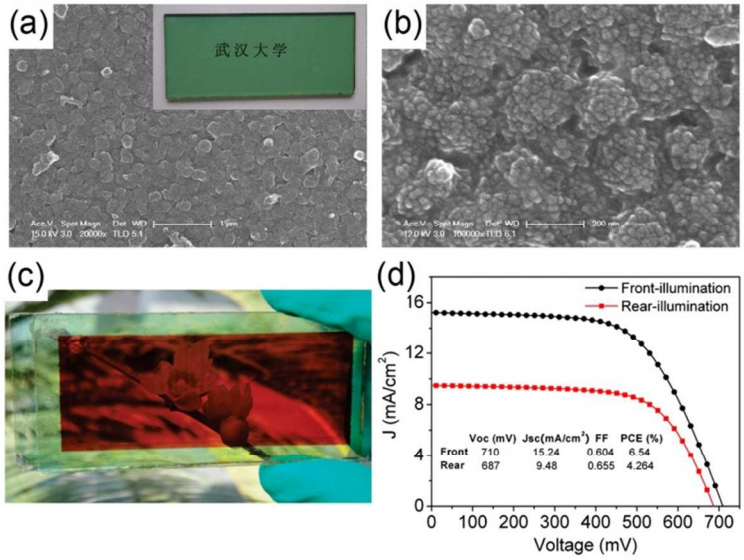

Fig. 6 SEM images of PANI film at (a) low magnification (inset is the photo of transparent PANI film grown on FTO glass), (b) high magnification; (c) photo of a bifacially active transparent DSC based on transparent PANI CE and (d) the corresponding J-V curves under front- and rear-side illuminations. Adapted with permission from ref 17. Copyright (2011) American Chemical Society.

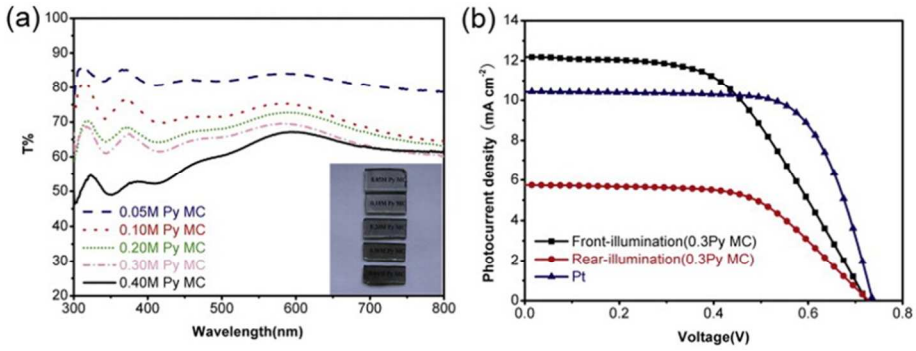

Fig. 7 (a) Transmittance of the PPy films prepared with different initial monomer concentrations, (b) J-V curves of DSCs using transparent PPy CE (prepared with 0.3M monomer concentration) and Pt CE. Adapted with permission from ref 18. Copyright (2013) Elsevier.

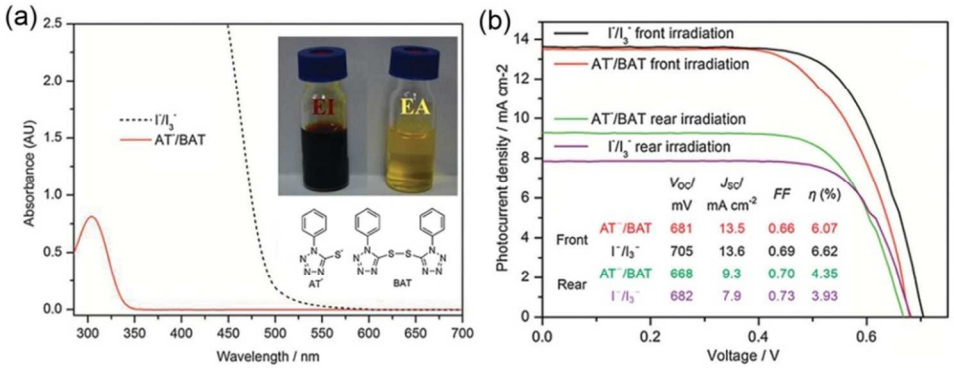

Fig. 8 (a) Absorption of AT^-/BAT and I^-/I_3^- based electrolytes, (b) J-V curves of bifacial DSCs using transparent PEDOT CEs based on AT^-/BAT and I^-/I_3^- based electrolytes. Adapted from ref 62.

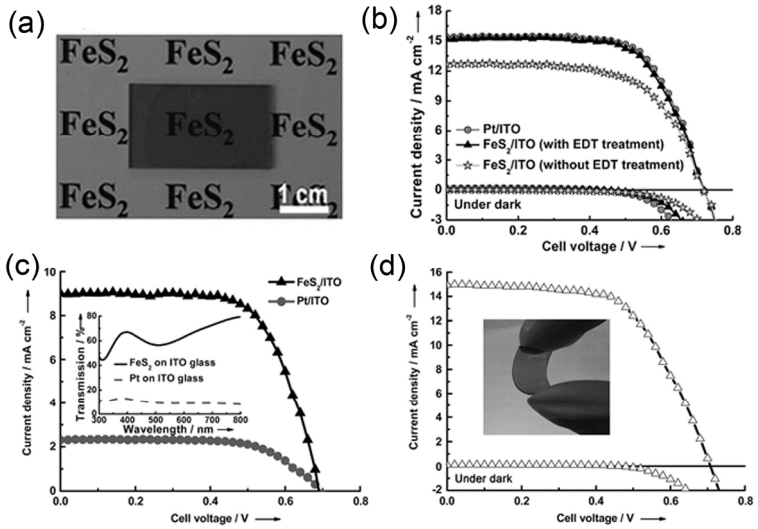

Fig.9 (a) Photo of FeS_2 thin film, J-V curves of DSCs using Pt and FeS_2 CEs under (b) front-side illumination and (c) rear-side illumination, (d) J-V curve of DSC using FeS_2 CE deposited on ITO/PET substrate. Adapted with permission from ref 72. Copyright (2013) Wiley-VCH.Verlag GmbH & Co. KGaA, Weinheim.

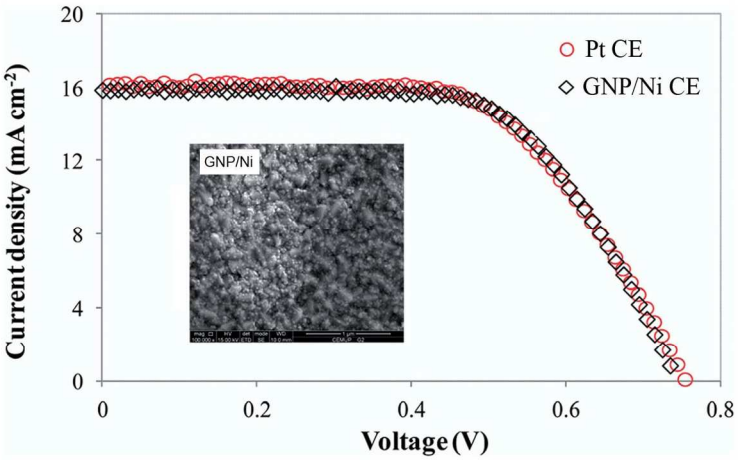

Fig. 10 J-V characteristics of DSCs using GNP/Ni CE (prepared from water) and Pt CE, the inset is the SEM image of GNP/Ni CE in which the Ni particles can be directly seen through the thin graphene layer. Adapted from ref. 78

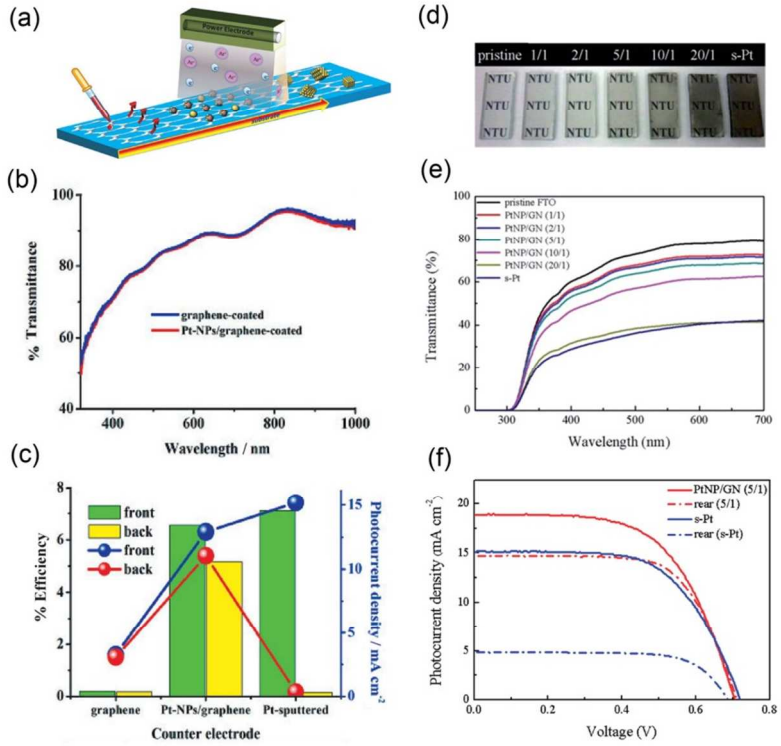

Fig. 11 (a) Illustration of the synthesis procedure of graphene/Pt composite CE using DPR, (b) Transmittance of graphene and graphene/Pt films on FTO, (c) Photovoltaic performance of bifacial DSCs using Pt, graphene, and graphene/Pt CEs. (Adapted with permission from ref. 83, copyright (2013) Wiley-VCH.Verlag GmbH & Co. KGaA, Weinheim.), (d) photographs and (e) transmittance of GNP/Pt CEs with different weight ratio of Pt and GNP, (f) J-V characteristics of bifacial DSCs using GNP/Pt (1/5) and Pt CEs under front- and rear-side illumination. Adapted from ref. 84.

Table 1 Summary of different transparent counter electrodes and their performance in bifacial dye-sensitized solar cells.

Counter Electrodes	T_{550}	Redox couple	PCE_{front}	PCE_{rear}	PCE_{rear}/PCE_{front}	PCE_{front}/PCE_{Pt}[a]	Ref.
Chemically assembled SWNTs	0.78	$Co(bpy)_3^{3+/2+}$	4.81 %	4.56 %	0.95	0.88	34
N-doped graphene	0.77	I_3^-/I^-	6.12 %	5.23 %	0.85	0.89	36
Pyrolytic carbon	0.7	I_3^-/I^-	6.07 %	5.04 %	0.83	0.88	43
PANI	0.7	I_3^-/I^-	6.7 %	4.15%	0.62	0.98	10
PANI (no FTO)	0.6	I_3^-/I^-	5.5 %	2.67 %	0.49	0.84	46
PANI	0.6	I_3^-/I^-	6.54 %	4.26 %	0.65	0.98	17
PANI	0.7	I_3^-/I^-	6.7 %	4.63 %	0.69	0.82	77
PPy	0.65	I_3^-/I^-	5.74 %	3.06 %	0.53	0.85	18
PEDOT	0.95	AT^-/BAT	6.07 %	4.35 %	0.72	3.97[b]	62
PEDOT/PSS on Ag network	0.6	I_3^-/I^-	1.02 %[c]	0.61 %	0.60	0.19	64
FeS	0.6	I_3^-/I^-	7.31 %	4.17 %	0.57	0.97	72
CoS	0.65	I_3^-/I^-	5.88 %	3.84 %	0.65	0.96	87
PANI/RGO	0.9	I_3^-/I^-	7.84 %	6.08 %	0.78	0.96	77
Graphene/Pt	0.8	I_3^-/I^-	6.55 %	5.17 %	0.79	0.92	83
GNP/Pt	0.7	I_3^-/I^-	8 %	7.01 %	0.88	1.12	84
PANI/Pt (on FTO)	0.7	I_3^-/I^-[d]	6.34 %	3.85 %	0.61	1.06	80
PANI/Pt (on ITO/PET)	0.7	I_3^-/I^-	5.4 %	4.0 %	0.74	1.06	86
CoS/Pt	0.8	I_3^-/I^-	6.15 %	4.45 %	0.72	1	87

[a] PCE_{front}/PCE_{pt} is defined as the ratio of the front-illuminated PCE of DSCs using non-Pt CEs and Pt CE under the same test condition, which is an important parameter to evaluate the performance of non-Pt CEs.

[b]The reference Pt CE showed very poor catalytic activity towards AT^-/BAT redox couple, which only exhibited a PCE of 1.53 %.

[c]The PCE_{front} was improved to 5.13% when TiO_2 NPs were incorporated into the PEDOT film.

[d] Quasi solid state electrolyte based on PVDF-HFP/TiO_2 was used.

TOC Figure

In this feature article, we pay a special attention to the recent advances in the development of Pt-free transparent CEs and highlight their applications in bifacial DSCs.